

Gravitational Waves from Periodic Three-Body Systems

V. Dmitrašinović and Milovan Šuvakov

Institute of Physics Belgrade, University of Belgrade, Pregrevica 118, 11080 Beograd, Serbia

Ana Hudomal

Fizički fakultet, University of Belgrade, Studentski Trg 12, 11000 Belgrade, Serbia

Three bodies moving in a periodic orbit under the influence of Newtonian gravity ought to emit gravitational waves. We have calculated the gravitational radiation quadrupolar waveforms and the corresponding luminosities for the 13+11 recently discovered three-body periodic orbits in Newtonian gravity. These waves clearly allow one to distinguish between their sources: all 13+11 orbits have different waveforms and their luminosities (evaluated at the same orbit energy and body mass) vary by up to 13 orders of magnitude in the mean, and up to 20 orders of magnitude for the peak values.

PACS numbers: 04.30.Db, 04.25.Nx, 95.10.Ce, 95.30.Sf

Keywords: gravitation; gravitational waves; celestial mechanics; three-body systems in classical mechanics

Direct detection of gravitational waves [1, 2] ought to come about in the foreseeable future, due to the substantial effort made at the operational and/or pending detectors. One of the most promising candidates for astrophysical sources of gravitational waves are the coalescing, i.e., inspiraling and finally merging binary compact stars [3, 4]. Binary coalescence is the only source for which there is a clear prediction of the signal and an estimate of the detection distance limit, as general relativists have completed numerical simulations of mergers of compact binaries, such as neutron stars and/or black holes, Refs. [5–7].

Slowly changing, quasiperiodic two-body orbits are weak sources of gravitational radiation, Refs. [8, 9]—only accelerated collapse leads to an increase in energy loss. The major part of the emitted energy in a binary coalescence comes from the final merger of two neutron stars, or black holes, that produces an intense burst of gravitational radiation. Of course, such mergers are one-off events, never to be repeated in the same system, so their detection is subject to their (poorly known) distribution in our Galaxy. It is therefore interesting to look for periodic sources of intense gravitational radiation.

There is now a growing interest in three-body systems as astrophysical sources of gravitational waves, Refs. [10–12]. These early works did not find a substantial increase in the luminosity (emitted power) from representative three-body orbits belonging to three families that were known at the time, Refs. [13–22], over the luminosity from a comparable periodic two-body system [27]. The luminosity of a (quadrupolar) gravitational wave is proportional to the square of the third time derivative of the quadrupole moment, see Refs. [8, 9], which, in turn, is sensitive to close approaches of two bodies in a periodic orbit [28]. Thus, getting as close as possible to a two-body collision without actually being involved in one, is a desirable property of the radiating system.

Recently 13 new distinct periodic orbits belonging to 12 (new) families have been discovered in Ref. [23], as well as 11 “satellite orbits” in the figure-eight family [24].

Some of these three-body orbits pass very close to binary collisions and yet avoid them, so they are natural candidates for periodic sources of intense gravitational radiation.

In this Letter we present our calculations of quadrupolar waveforms, Fig. 1, and of luminosities, see Table I and Fig. 2 of gravitational radiation emitted by the 13+11 recently discovered periodic three-body gravitating orbits, Refs. [23, 24]. We have also calculated waveforms of all published Broucke-Hadjidemetriou-Henon (BHH) orbits [14–20], which we omit from this Letter for the sake of brevity, and because they are closely related to Henon’s “criss-cross” one, studied in Ref. [10]. The waves of the 13+11 new orbits show clear distinctions in form and luminosity, thus ensuring that they would be distinguishable (provided their signals are strong enough to be detected).

We consider systems of three equal massive particles moving periodically in a plane under the influence of Newtonian gravity. The quadrupole moment I_{ij} of three bodies with equal masses $m_n = m$, ($n = 1, 2, 3$) is expressed as $I_{ij} = \sum_{n=1}^3 m x_n^i x_n^j$, where x_n^i is the location of n th body, and the spatial dimension indices i and j run from 1 to 3 (with $x^1 = x$, $x^2 = y$, $x^3 = z$). The reduced quadrupole Q_{ij} is defined as $Q_{ij} = I_{ij} - \frac{1}{3}\delta_{ij} \sum_{k=1}^3 I_{kk}$. The gravitational waveforms denoted by h_{ij}^{TT} are, asymptotically,

$$h_{ij}^{TT} = \frac{2G}{rc^4} \frac{d^2 Q_{ij}}{dt^2} + \mathcal{O}\left(\frac{1}{r^2}\right), \quad (1)$$

where r is the distance from the source, Refs. [8, 9]. Here, TT means (i) transverse ($\sum_{i=1}^3 h_{ij}^{TT} \hat{n}^i = 0$) and (ii) traceless ($\sum_{i=1}^3 h_{ii}^{TT} = 0$), where \hat{n}_i denotes the unit vector of the gravitational wave’s direction of propagation. The two independent waveforms $h_{+, \times}$ of a quadrupolar gravitational wave propagating along the z axis, Refs. [8, 9]

TABLE I: Initial conditions and periods of three-body orbits. $\dot{x}_1(0)$, $\dot{y}_1(0)$ are the first particle’s initial velocities in the x and y directions, respectively, T is the period of the (rescaled) orbit to normalized energy $E = -1/2$, Θ is the rotation angle (in radians) and $\langle P \rangle$ is the mean luminosity (power) of the waves emitted during one period. Other two particles’ initial conditions are specified by these two parameters, as follows: $x_1(0) = -x_2(0) = -\lambda$, $x_3(0) = 0$, $y_1(0) = y_2(0) = y_3(0) = 0$, $\dot{x}_2(0) = \dot{x}_1(0)$, $\dot{x}_3(0) = -2\dot{x}_1(0)$, $\dot{y}_2(0) = \dot{y}_1(0)$, $\dot{y}_3(0) = -2\dot{y}_1(0)$. The Newtonian coupling constant G is taken as $G = 1$ and the masses are equal $m_{1,2,3} = 1$.

Name	$\dot{x}_1(0)$	$\dot{y}_1(0)$	λ	T	$\Theta(\text{rad})$	$\langle P \rangle$
Moore’s figure eight	0.216 343	0.332 029	2.574 29	26.128	0.245 57	1.35×10^0
Simo’s figure eight (M8) ⁷	0.211 139	0.333 568	2.583 87	26.127	0.277 32	1.36×10^0
I.A.1 butterfly I	0.147 262	0.297 709	3.008 60	182.873	0.269 21	2.46×10^0
I.A.2 butterfly II	0.147 307	0.060 243	4.340 39	56.378	0.034 78	1.35×10^5
I.A.3 bumblebee	0.196 076	0.048 69	4.016 39	56.375	0.066 21	5.52×10^6
I.B.1 moth I	0.111 581	0.355 545	2.727 51	286.192	-1.090 4	1.01×10^5
I.B.2 moth II	0.279 332	0.238 203	2.764 56	68.464	0.899 49	5.25×10^2
I.B.3 butterfly III	0.271 747	0.280 288	2.611 72	121.006	1.138 78	1.87×10^3
I.B.4 moth III	0.211 210	0.119 761	3.693 54	98.435	0.170 35	3.53×10^5
I.B.5 goggles	0.212 259	0.208 893	3.263 41	152.330	0.503 01	7.48×10^5
I.B.6 butterfly IV	0.037 785	0.058 010	4.860 23	112.129	-0.406 17	1.33×10^4
I.B.7 dragonfly	0.170 296	0.038 591	4.226 76	690.632	0.038 484	1.23×10^{13}
II.B.1 yarn	0.047 479	0.346 935	2.880 67	104.005	-0.406 199	1.25×10^6
II.C.2a yin-yang I	0.361 396	0.225 728	2.393 07	205.469	-1.015 61	2.33×10^6
II.C.2b yin-yang I	0.304 003	0.180 257	2.858 02	83.727	0.659 242	1.31×10^5
II.C.3a yin-yang II	0.143 554	0.166 156	3.878 10	83.727	-0.020 338	1.31×10^5
II.C.3b yin-yang II	0.229 355	0.181 764	3.302 84	334.877	0.472 891	7.19×10^{10}
II.C.3b yin-yang II	0.227 451	0.170 639	3.366 76	334.872	0.254 995	7.19×10^{10}

can be expressed as

$$h_+ = \frac{2G}{c^4 r} \sum_{i=1}^3 m_i (\dot{x}_i^2 + x_i \ddot{x}_i - \dot{y}_i^2 - y_i \ddot{y}_i), \quad (2)$$

$$h_\times = \frac{2G}{c^4 r} \sum_{i=1}^3 m_i (\ddot{x}_i y_i + 2\dot{x}_i \dot{y}_i + x_i \ddot{y}_i), \quad (3)$$

where r denotes the distance from the source to the observer. We set the units of $G = c = m = 1$ throughout this Letter.

Here the coordinate axes x and y are chosen so that they coincide with the orbits’ two (reflection) symmetry axes, when they exist, i.e., when the orbits are from class I, as defined in Ref. [23]. Otherwise, e.g., when only a single point reflection symmetry exists, as in class II orbits, the x , y axes are taken to be the eigenvectors of the moment-of-inertia tensor. The rotation angle necessary for each orbit to be aligned with these two axes is given in Table I [29].

The first gravitational radiation waveforms for periodic three-body systems were studied in Refs. [10–12]. They calculated the quadrupole radiation waveforms for three periodic orbits of the following three-equal-mass systems: (i) of the Lagrange “equilateral triangle” orbit [13], (ii) of Henon’s “criss-cross” [19], and (iii) of Moore’s “figure eight” [21]. These three orbits are characteristic representatives of the (only) three families of periodic three-body orbits known at the time. Reference [10] found distinct gravitational waveforms for each of the three families, thus suggesting that one might be able to distinguish

between different three-body systems as sources of gravity waves by looking at their waveforms [30].

In the meantime 13+11 new orbits belonging to 12 new families have been found, Refs. [23, 24]. The families of three-body orbits can be characterized by their topological properties viz. the conjugacy classes of the fundamental group, in this case, the free group on two letters (a, b) , Ref. [25]. The free group element tells us the number of times the system’s trajectory on the shape sphere passes around one or another (prechosen) two-body collision point within one period. Every time the system is close to a two-body collision the (relative) velocities, accelerations, and the third derivatives of relative coordinates increase, so that the luminosity of gravitational radiation also increases; i.e., there is a burst of gravitational radiation. This argument can be made more quantitative by appealing to two-body results of Ref. [8], as is shown in footnote [32].

We show the gravitational radiation waveforms $h_{+, \times}$ in Fig. 1, emitted by three massive bodies moving according to the orbits from Refs. [23, 24] belonging to these families, where Eqs. (2) and (3) are used as the definitions of the two waveforms.

First, we note that all of the calculated three-body orbits’ waveforms are distinct [31], thus answering (in the positive) the question about their distinguishability posed in Ref. [10]. In Fig. 1 we also show the gravitational waveform of one “old” orbit: Simo’s figure eight, (discovered in 2002) belonging to the figure-eight family. Simo’s figure eight is an important example, as it is virtually indistinguishable from Moore’s one, and yet

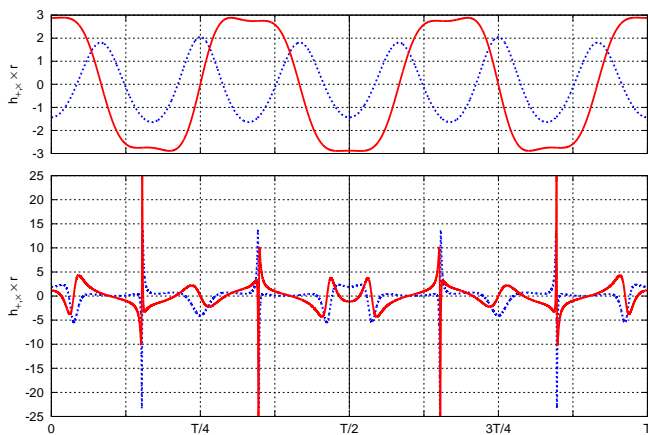


FIG. 1: The gravitational radiation quadrupolar waveforms $h_{+,x} \times r$ as functions of the elapsed time t in units of the period T , for two periodic three-body orbits (in units of Gm/c^2 ; we have set $G = m = c = 1$ throughout this Letter) and r is the radial distance from the source to the observer. Dotted (blue) and solid (red) curves denote the $+$ and \times modes, respectively. Top: Simo's figure eight, Ref. [22]; and bottom: orbit I.B.1 Moth I. Note the symmetry of these two graphs under the (time-)reflection about the orbits' midpoint $T/2$ during one period T .

the two have distinct gravitational waveforms, see our Fig. 1 and Fig. 2 in Ref. [10]. That is so because these two figure-eight solutions have distinct time dependences of the hyperradius R , where $R^2 \sim (1/m)\delta_{ij} \sum_{k=1}^3 I_{kk}$, so that the two orbits have different quadrupolar waveforms.

Note, moreover, the symmetry of the waveforms in Fig. 1 with respect to reflections of time about the midpoint of the period $T/2$: this is a consequence of the special subset of initial conditions (vanishing angular momentum and passage through the Euler point on the shape sphere) that we used. There are periodic three-body orbits, such as those from the BHH family, that do not have this symmetry.

The gravitational waveforms' maxima range from 20 to 50 000 in our units, with the energy fixed at $E = -1/2$. This large range of maximal amplitudes is due to the differences in the proximity of the approach to two-body collisions in the corresponding orbits. One can explicitly check that the bursts of gravitational radiation during one period correspond to close two-body approaches.

As stated above, the (negative) mean power loss $\langle dE/dt \rangle$ of the three-body system, or the (positive) mean luminosity (emitted power) of quadrupolar gravitational radiation $\langle P \rangle$, averaged over one period, is proportional to the square of the third time derivative of the (reduced) quadrupole moment $Q_{jk}^{(3)}$, $\langle dE/dt \rangle = -\langle P \rangle = -\frac{1}{5}(G/c^5) \sum_{j,k=1}^3 \langle Q_{jk}^{(5)} \dot{Q}_{jk} \rangle = -\frac{1}{5}(G/c^5) \sum_{j,k=1}^3 \langle Q_{jk}^{(3)} Q_{jk}^{(3)} \rangle$, (for an original derivation see Refs. [8, 9], for pedagogical ones, see Refs. [1, 2]). But, $Q_{jk}^{(3)}$ are proportional to the first time derivatives

of the gravitational waveforms $Q_{jk}^{(3)} = (d/dt)Q_{jk}^{(2)} \propto (d/dt)h_{+,x}$. The peak amplitudes of gravitational waveforms $h_{+,x}$, in turn, grow in the vicinity of two-body collisions [32], which explains the burst of gravitational radiation as one approaches a two-body collision point.

The mean and instantaneous luminosities, expressed in our units, of these orbits, normalized to $E = -1/2$, are shown in Table I and Fig. 2, respectively. Note that in Table I we show only three of the 11 orbits belonging to the figure-eight family: Moore's, Simo's, and the stable choreography (M8)⁷; they have all the same order of magnitude of the mean luminosity [33], whereas the butterfly I and butterfly II orbits, which belong to the same topological family, have mean luminosities that differ by more than a factor of 40.

Generally, the mean luminosities of these 24 orbits cover 13 orders of magnitude, ranging from 1.35 (Moore's figure eight) to 1.23×10^{13} (I.B.6 butterfly IV) in our units; see Table I. The peak instantaneous luminosities have an even larger range: 20 orders of magnitude; see Fig. 2. Here, the symmetric form of the instantaneous (time unaveraged) power $P = \frac{1}{5}(G/c^5) \sum_{j,k=1}^3 Q_{jk}^{(3)} \dot{Q}_{jk}^{(3)}$ was used. This gives us hope that at least some of these three-body periodic orbits can, perhaps, lead to detectable gravitational radiation signals.

It is a different question if some or all of these sources of gravitational radiation would be observable by the present-day and the soon-to-be-built gravitational wave detectors: that strongly depends on the absolute values of the masses, velocities, and the average distances between the three celestial bodies involved, as well as on the distribution of such sources in our Galaxy.

Moreover, note that all of the newly found and analyzed three-body orbits have zero angular momentum, and many of them are unstable. It is well known [16–20] that by changing the angular-momentum within the same family of three-body orbits, the stability of an orbit changes as well. So, it may happen that a previously stable orbit turns into an unstable one, and vice versa. For this reason it should be clear that a careful study of gravitational-radiation-induced energy- and angular-momentum dissipation is necessary for these orbits [34]. Moreover, if realistic results are to be obtained, post-Newtonian approximations will have to be applied in the future. Such relativistic corrections are most important at large velocities, i.e., precisely near close approaches that are so crucial for large gravitational radiation. Thus, the present Letter is meant only to highlight the possibilities in this field, and should be viewed as an invitation to join in the more realistic future studies.

V. D. and M. Š. were financially supported by the Serbian Ministry of Science and Technological Development under Grants No. OI 171037 and No. III 41011. A. H. was supported by the City of Belgrade studentship (Gradska stipendija grada Beograda) during the year 2012–2013, and was a recipient of the “Dositeja” stipend for the year 2013–2014, from the Fund for Young Talents (Fond za mlade talente - stipendija “Dositeja”) of the

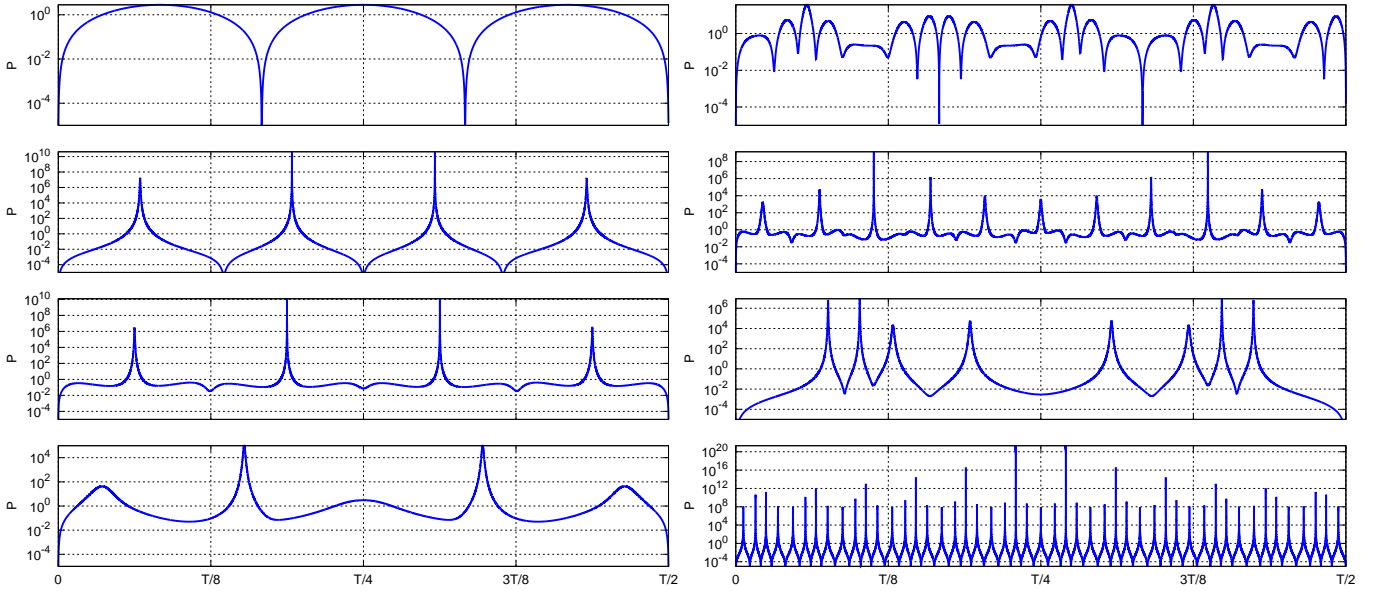


FIG. 2: The instantaneous (time unaveraged) luminosity P of quadrupolar gravitational radiation emitted from periodic three-body orbits as a function of the elapsed time t in units of the period T . Note the logarithmic scale for the luminosity P (y axis). Top left: Moore's figure eight; second from top left: I.A.2 butterfly II; third from top left: II.B.7 dragonfly; bottom left: I.B.1 moth I; top right: $(M8)^7$; second from top right: I.A.3 bumblebee; second from bottom right: I.B.5 goggles; bottom right: II.B.6 butterfly IV.

Serbian Ministry for Youth and Sport.

-
- [1] C. W. Misner, K. S. Thorne, and J. A. Wheeler, *Gravitation* (Freeman, San Francisco, CA, 1973).
- [2] A.P. Lightman, W.H. Press, R.H. Price, and S.A. Teukolsky, *Problem Book in Relativity and Gravitation* (Princeton University Press, NJ, Princeton 1975).
- [3] C. Cutler *et al.*, Phys. Rev. Lett. **70**, 2984 (1993).
- [4] C. Cutler and K. S. Thorne, in *General Relativity and Gravitation: Proceedings of the 16th International Conference*, edited by N. T. Bishop and S. D. Maharaj (World Scientific, Singapore, 2002), p. 72.
- [5] M. Campanelli, C. O. Lousto, P. Marronetti, and Y. Zlochower, Phys. Rev. Lett. **96**, 111101 (2006).
- [6] J. G. Baker, J. Centrella, D.-I. Choi, M. Koppitz, and J. van Meter, Phys. Rev. Lett. **96**, 111102 (2006).
- [7] F. Pretorius, Phys. Rev. Lett. **95**, 121101 (2005).
- [8] P. C. Peters and J. Mathews, Phys. Rev. **131**, 435 (1963).
- [9] P. C. Peters, Phys. Rev. **136**, B1224 (1964).
- [10] Y. Torigoe, K. Hattori, and H. Asada, Phys. Rev. Lett. **102**, 251101 (2009).
- [11] T. Chiba, T. Imai, and H. Asada, Mon. Not. R. Astron. Soc. **377**, 269 (2007).
- [12] H. Asada, Phys. Rev. D **80**, 064021 (2009).
- [13] J. L. Lagrange, Miscellanea Taurinensia **4**, 118 (1772); Oeuvres **2**, 67; Mécanique Analytique, 262; 2nd ed. **2**, 108; Oeuvres **12**, 101.
- [14] R. Broucke and D. Boggs, Celest. Mech. **11**, 13 (1975).
- [15] R. Broucke, Celest. Mech. **12**, 439 (1975).
- [16] J.D. Hadjidemetriou, Celest. Mech. **12**, 155 (1975).
- [17] J.D. Hadjidemetriou and Th. Christides, Celest. Mech. **12**, 175 (1975).
- [18] J.D. Hadjidemetriou, Celest. Mech. **12**, 255 (1975).
- [19] M. Henon, Celest. Mech. **13**, 267 (1976).
- [20] M. Henon, Celest. Mech. **15**, 243 (1977).
- [21] C. Moore, Phys. Rev. Lett. **70**, 3675 (1993).
- [22] C. Simó, in *Celestial Mechanics*, edited by A. Chenciner, R. Cushman, C. Robinson, and Z. J. Xia (Am. Math. Soc., Providence, RI, 2002).
- [23] Milovan Šuvakov and V. Dmitrašinović, Phys. Rev. Lett. **110**, 114301 (2013).
- [24] M. Šuvakov, Celest. Mech. Dyn. Astron. **119**, 369 (2014).
- [25] M. Šuvakov and V. Dmitrašinović, Am. J. Phys. **82**, 609 (2014).
- [26] M. R. Janković and M. Šuvakov (to be published).
- [27] The question of distinguishability between various three-body and two-body sources' of gravitational radiation was also raised in Ref. [10].
- [28] The proximity to a two-body collision can be defined mathematically by using the so-called hyperspherical variables, and the shape-sphere variables, in particular; see Refs. [23, 25]. Of course, it is not just the proximity

to the two-body collision point that is driving this surge of emitted power, but also the accompanying increase in the velocities, accelerations, and third derivatives of the relative positions; see the text below.

- [29] When the orbit passes through the Euler point twice, such as in the yin-yang orbits, there are two different sets of initial conditions, and, consequently, two different rotation angles—we indicate exactly which one of the two solutions is taken. The total energy has been scaled to $E = -1/2$ for all solutions, so as to provide a meaningful comparison of peak amplitudes and luminosities.
- [30] A more detailed study of the waveforms emanating from the Lagrangian three-body orbit can be found in Ref. [12].
- [31] We do not show these waveforms here, except for the two in Fig. 1, for brevity's sake, and because many are fairly similar to the second waveform in Fig. 1—regular sequences of spikes.
- [32] The following argument was suggested by one of the referees: If a section of the trajectory of two bodies (within a three-body system) that approach a two-body collision can be approximated by an ellipse, then the luminosity P is proportional to $P \sim (1 - e^2)^{-7/2}$, see Eq. (5.4) in Ref. [9], where e is the eccentricity of the ellipse. Therefore, P grows without bounds as $e \rightarrow 1$, i.e., as the orbit approaches a two-body collision.
- [33] Note that the figure-eight family members have, on the average, the lowest luminosity among the orbits considered here.
- [34] We plan to do such a study, which cannot be completed, however, without an extension of each orbit to a family of orbits with nonvanishing angular momenta. So far, only the BHH family has been extended in such a way, but even that one case is not complete [26].